Supplementary data

The ssDNA-binding protein MEIOB acts as a dosage-sensitive regulator of meiotic recombination

Rui Guo, Yang Xu, N Adrian Leu, Lei Zhang, Serge Y Fuchs, Lan Ye, & P Jeremy Wang

Summary:

2 supplementary tables

10 supplementary figures

Supplementary Table S1. Primary antibodies used in this study

Antibody	Host	Producer	Cat. No/reference	Dilution	
				WB	IF
RPA2	Rabbit	Custom-made	(Ref. 7)	1:250	1:50
MEIOB	Rabbit/guinea pig	Custom-made	(Ref. 17)	1:2000	1:50
SPATA22	Rabbit	ProteinTech Group	16989-1-AP	1:200	1:50
TEX11	Rabbit	Custom-made	(Ref. 26)		1:50
γH2AX	Mouse	Millipore	05-636	1:2000	1:500
SYCP1	Rabbit	Abcam	Ab15090		1:100
SYCP3	Mouse	Abcam	Ab97672	1:3000	1:200
SYCP3	Rabbit	ProteinTech Group	23024-1-AP		1:200
MLH1	Mouse	BD Biosciences	50838		1:25
HEI10	Rabbit	Abcam	Ab171035		1:25
H3S10ph	Rabbit	Cell Signaling Technology	9701S		1:200
MYC	Mouse	Clontech	631206	1:2000	
GFP	Rabbit	Abcam	Ab290	1:2000	
FLAG	Mouse	Sigma	F1804	1:5000	
ACTB	Mouse	Sigma	A5441	1:5000	
V5	Mouse	Invitrogen	R960-25	1:2000	
c-JUN	Rabbit	Cell Signaling Technology	9165T	1:1000	
LC3A/B	Rabbit	Cell Signaling Technology	12741T	1:1000	

Supplementary Table S2. Mating test results of adult males and females

A. Mating test result of adult males*

Genotype (Males)	Age (wk)	Length of mating (month)	No. of males	No. of litters/male (mean ± sd)	Fertility	Litter size (mean ± sd)
Meiob$^{N64I/+}$	7	3	4	3.50 ± 0.58	100% (4/4)	8.18 ± 1.51
Meiob$^{N64I/N64I}$	7	3	4	3.25 ± 0.50	100% (4/4)	8.32 ± 1.67
Meiob$^{N64I/\Delta S67}$	7	3	5	2.0 ± 0.0	60% (3/5) **	8.83 ± 2.25
Meiob$^{\Delta S67/\Delta S67}$	7	3	4	0	0% (0/4)	0

* Each male was housed with one wild type female for three months.
** Two males did not sire offspring.

B. Mating test result of adult females†

Genotype (females)	Age (wk)	Length of mating (month)	No. of females	No. of litters/female (mean ± sd)	Fertility	Litter size (mean ± sd)
Meiob$^{N64I/+}$	8	3	3	3.67 ± 0.58	100%	7.89 ± 1.76
Meiob$^{N64I/N64I}$	8	3	3	3.33 ± 0.58	100%	8.20 ± 1.65
Meiob$^{N64I/\Delta S67}$	8	3	3	3.0 ± 0.0	100%	7.80 ± 1.92
Meiob$^{\Delta S67/\Delta S67}$	8	3	3	0	0%	0

† Each female was housed with one wild type male for three months.

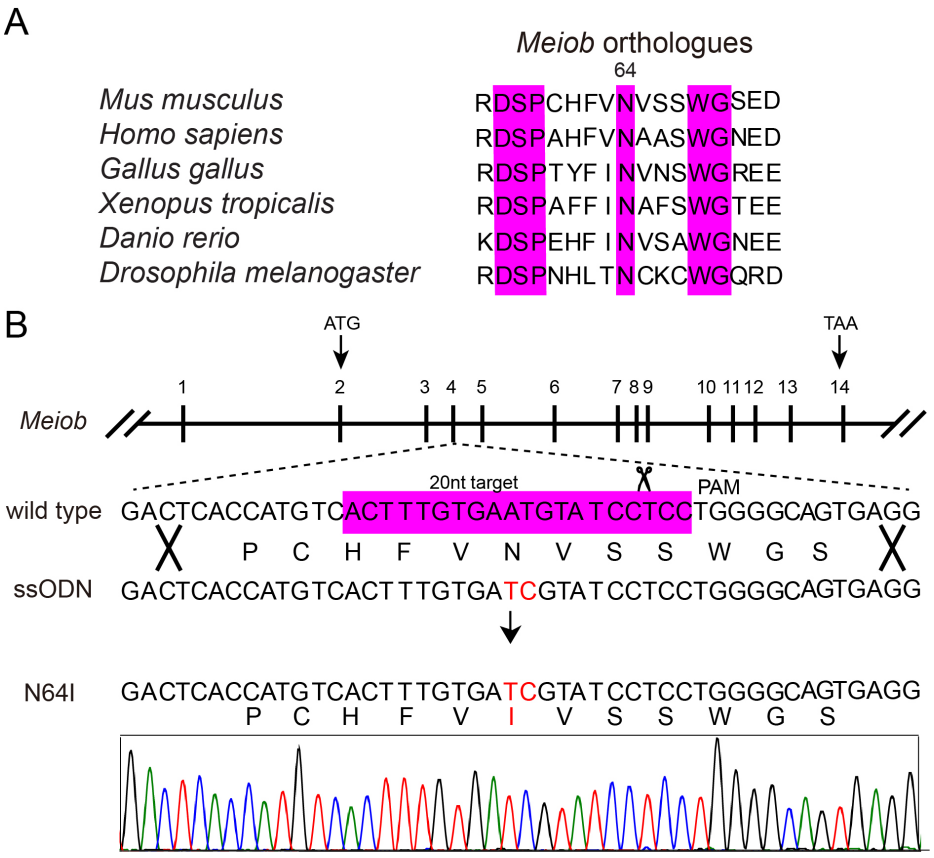

Supplementary Figure S1. CRISPR/Cas9-mediated generation of the *Meiob*^{N64I} mutation. (**A**) Conservation of asparagine 64 (N64) in MEIOB across species. (**B**) Diagram of *Meiob* alleles (wild type and N64I), sgRNA (in red), and single-stranded donor oligonucleotide DNA template (ssODN). The *Meiob*^{N64I} mutation was confirmed by sequencing.

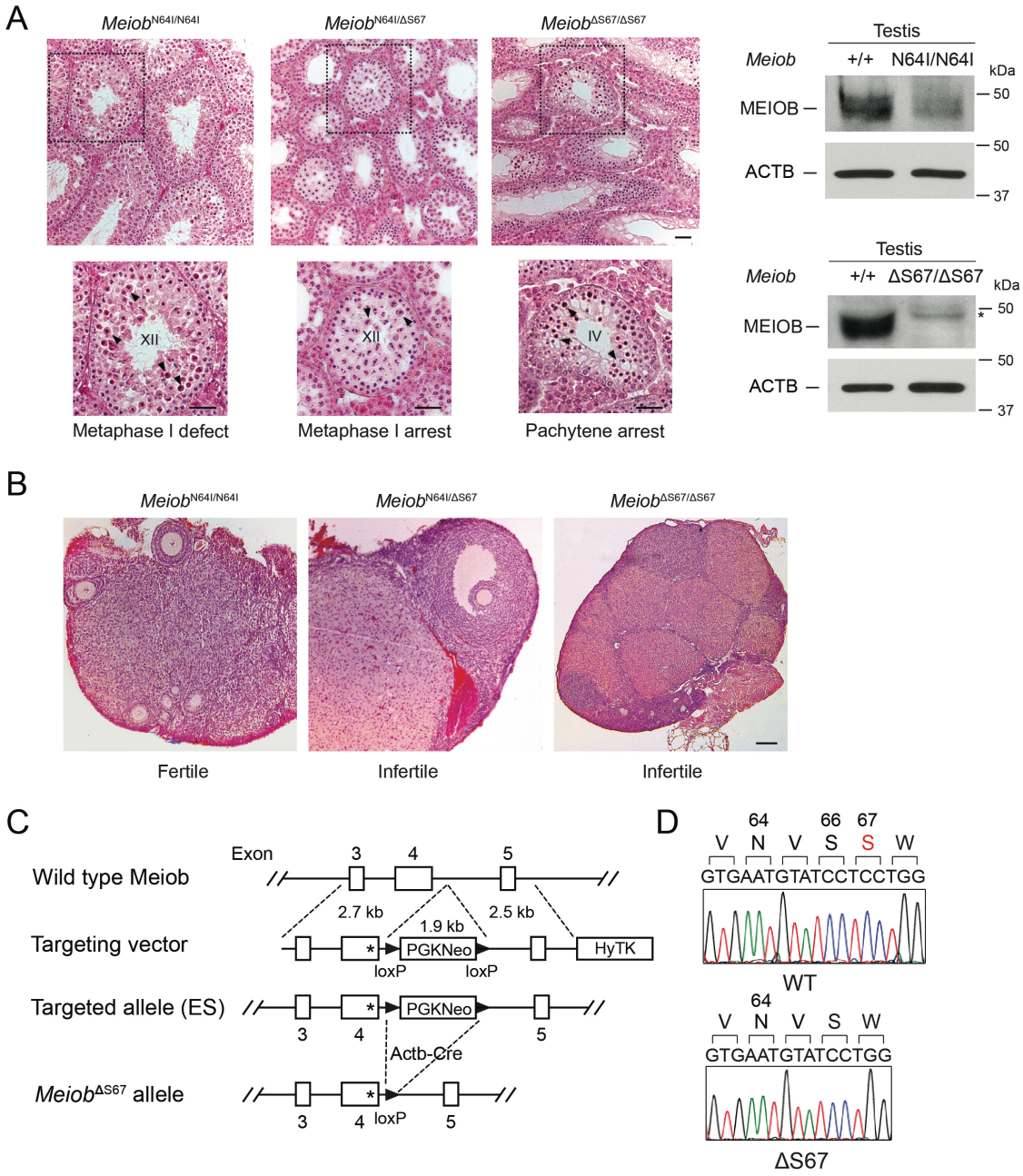

Supplementary Figure S2. Generation of the *Meiob*$^{\Delta S67}$ mutation through CRISPR/Cas9 and gene targeting in ES cells. (**A**) Histology of testes from 8-week-old founder mice generated through CRISPR/Cas9 injection of zygotes. Western blot analysis of MEIOB in testes is shown on the right. ACTB serves as a loading control. Scale bars, 50 µm. (**B**) Histology of ovaries from 8-week-old founder mice generated through CRISPR/Cas9 injection of zygotes. While the ovaries from *Meiob*$^{N64I/N64I}$ and *Meiob*$^{N64I/\Delta S67}$ founder females contained follicles, the ovary from *Meiob*$^{N64I/\Delta S67}$ founder females lacked oocytes. Scale bar, 50 µm. **(C)** Generation of the *Meiob*$^{\Delta S67}$ mutation through gene targeting in ES cells. Diagram of *Meiob* alleles. Codon 67 (Serine 67) lies in exon 4. Asterisk denotes the deletion of S67 (ΔS67). The neomycin selection marker PGKNeo is flanked by *loxP* sites. HyTK provides negative selection in ES cells by ganciclovir. **(D)** Sequencing confirmed the deletion of codon 67 in *Meiob*. The codons for S66 and S67 are identical (TCC). Because the S67 residue is more evolutionarily conserved than S66 (Supplementary Figure S1A), this deletion is referred to as ΔS67. Alternatively, this deletion can be called ΔS66.

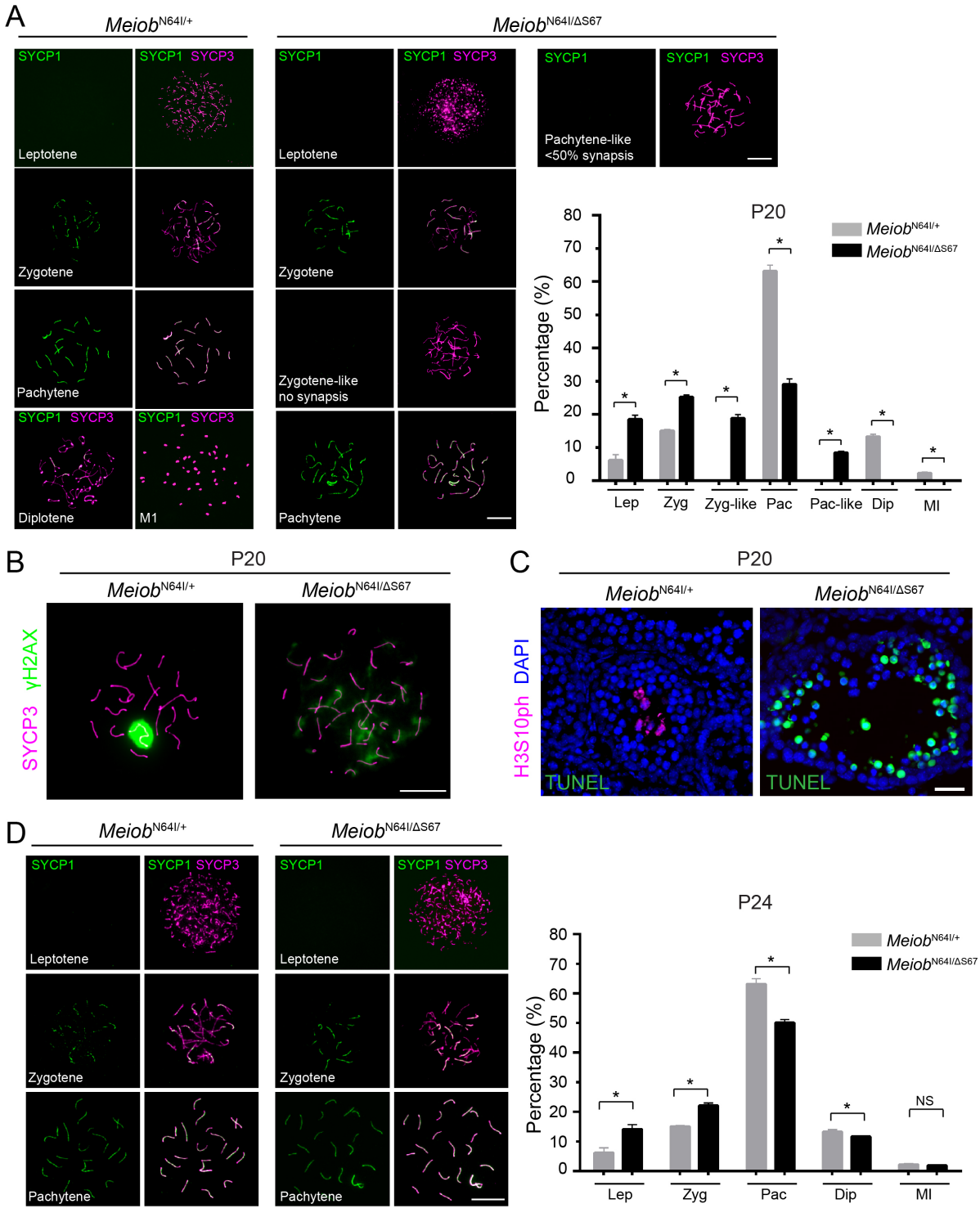

Supplementary Figure S3. The *Meiob*$^{N64I/\Delta S67}$ mice display defects in synapsis at P20 but not at P24. **(A)** Spread nuclei of spermatocytes from P20 *Meiob*$^{N64I/+}$ and *Meiob*$^{N64I/\Delta S67}$ males were immunostained with anti-SYCP1 and anti-SYCP3 antibodies. The graph shows the percentage of spermatocytes at each stage of meiotic prophase I. 181 *Meiob*$^{N64I/+}$ and 155 *Meiob*$^{N64I/\Delta S67}$ spermatocytes from three mice per genotype were counted. Data are presented as mean ± S.D., $*P < 0.05$ by Student's *t*-test. Scale bar, 10 μm. (**B**) Distribution of γH2AX in *Meiob*$^{N64I/+}$ and *Meiob*$^{N64I/\Delta S67}$ spermatocytes at P20. γH2AX was present in the chromatin of *Meiob*$^{N64I/\Delta S67}$ pachytene-like

spermatocytes. Scale bar, 10 μm. **(C**) TUNEL analysis of *Meiob*$^{N64I/+}$ and *Meiob*$^{N64I/\Delta S67}$ testes at P20. Scale bar, 20 μm. **(D**) Spread nuclei of spermatocytes from P24 *Meiob*$^{N64I/+}$ and *Meiob*$^{N64I/\Delta S67}$ males were immunostained with anti-SYCP1 and anti-SYCP3 antibodies. The graph shows the percentage of each type of spermatocytes. 212 *Meiob*$^{N64I/+}$ and 180 *Meiob*$^{N64I/\Delta S67}$ spermatocytes from three mice per genotype were counted. Data are presented as mean ± S.D., $*P < 0.05$ by Student's *t*-test. NS, non-significant. Lep, leptotene; Zyg, zygotene; Zyg-like, zygotene-like; Pac, pachytene; Pac-like, pachytene-like; Dip, diplotene; MI, metaphase I. Scale bar, 10 μm.

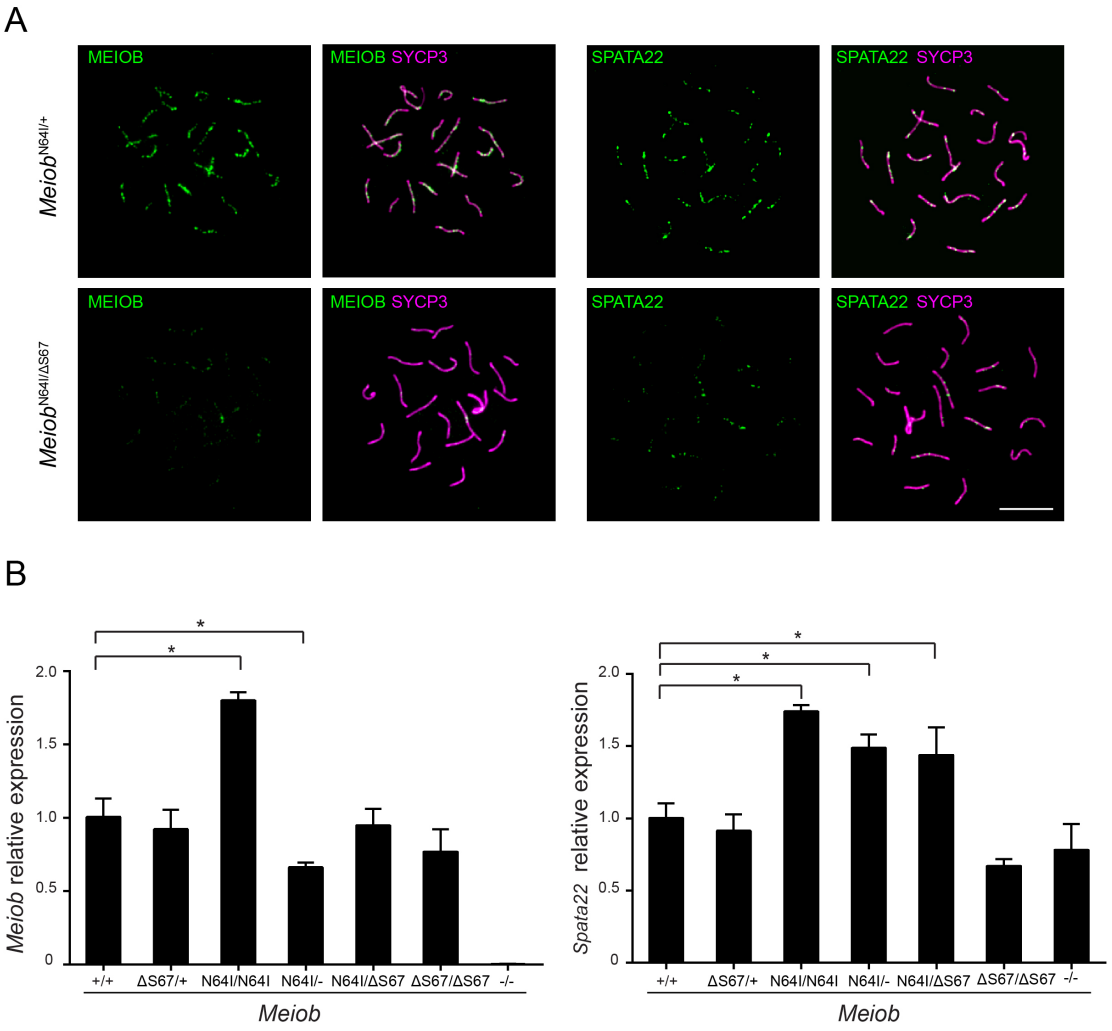

Supplementary Figure S4. Analysis of protein foci and transcript abundance of *Meiob* and *Spata22* in testes at P20. (**A**) Detection of MEIOB and SPATA22 foci on meiotic chromosomes at P20. The intensity of MEIOB and SPATA22 foci is weaker in *Meiob*$^{N64I/\Delta S67}$ spermatocytes than in *Meiob*$^{N64I/+}$ spermatocytes. Scale bar, 10 μm. (**B**) Real-time PCR quantitation of *Meiob* and *Spata22* transcripts in P20 testes (three mice per genotype were used). Related to Figure 4G. Data are presented as mean ± S.D., **P* < 0.05 by Student's *t*-test.

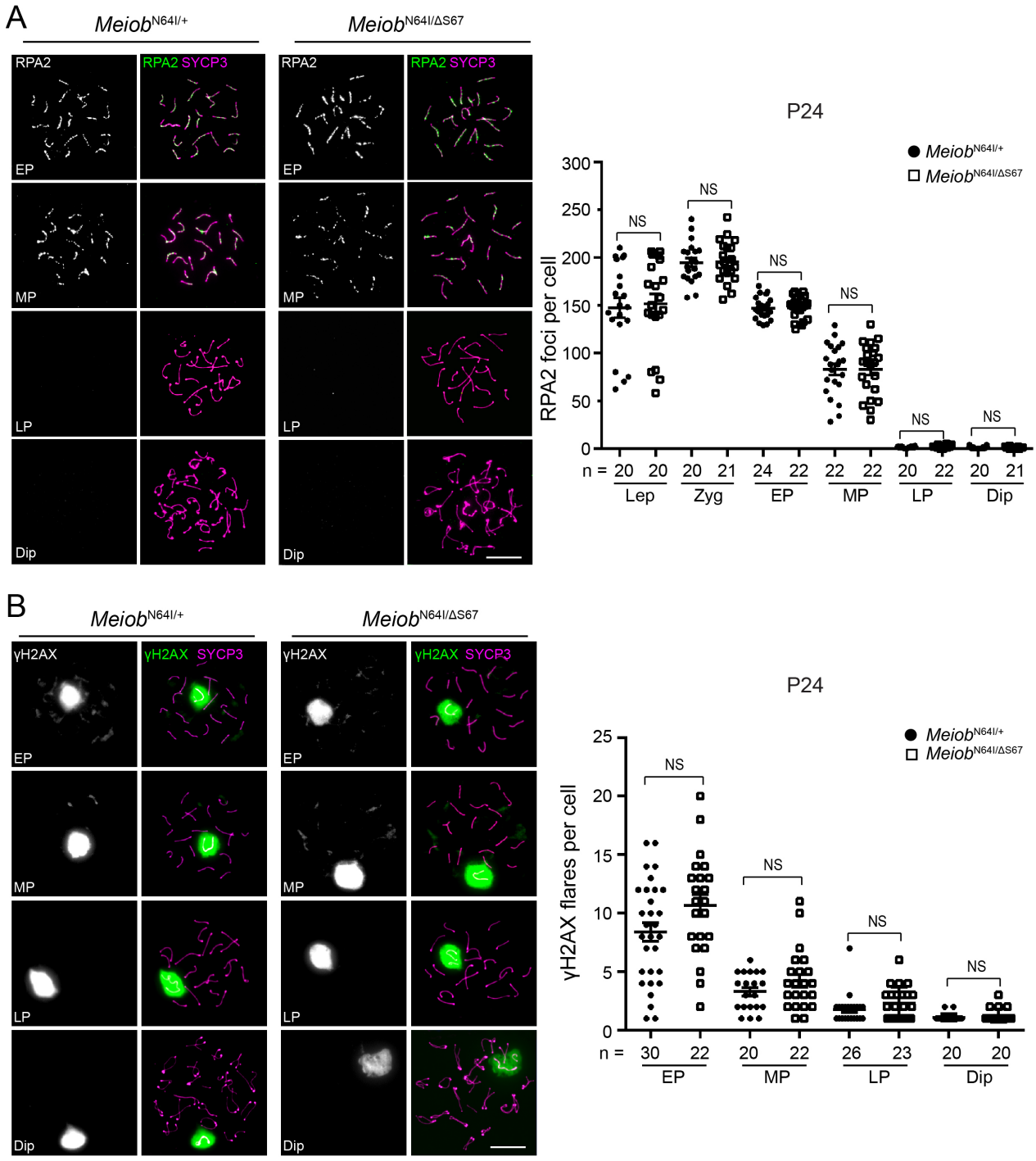

Supplementary Figure S5. Analysis of RPA2 and γH2AX in P24 *Meiob*$^{N64I/+}$ and *Meiob*$^{N64I/\Delta S67}$ spermatocytes. (**A**) Analysis of RPA2 foci in P24 spermatocytes. n, number of spermatocytes. Leptotene (Lep), Zygotene (Zyg), Early-pachytene (EP), Mid-pachytene (MP), late-pachytene (LP), Dip (Diplotene). **(B)** Analysis of γH2AX flares in P24 spermatocytes. The γH2AX in the XY body was counted once. n, number of spermatocytes. Three mice per genotype were analyzed. *$P < 0.05$ by Student's *t*-test. Early-pachytene (EP), Mid-pachytene (MP), late-pachytene (LP), Dip (Diplotene). Scale bars, 10 μm.

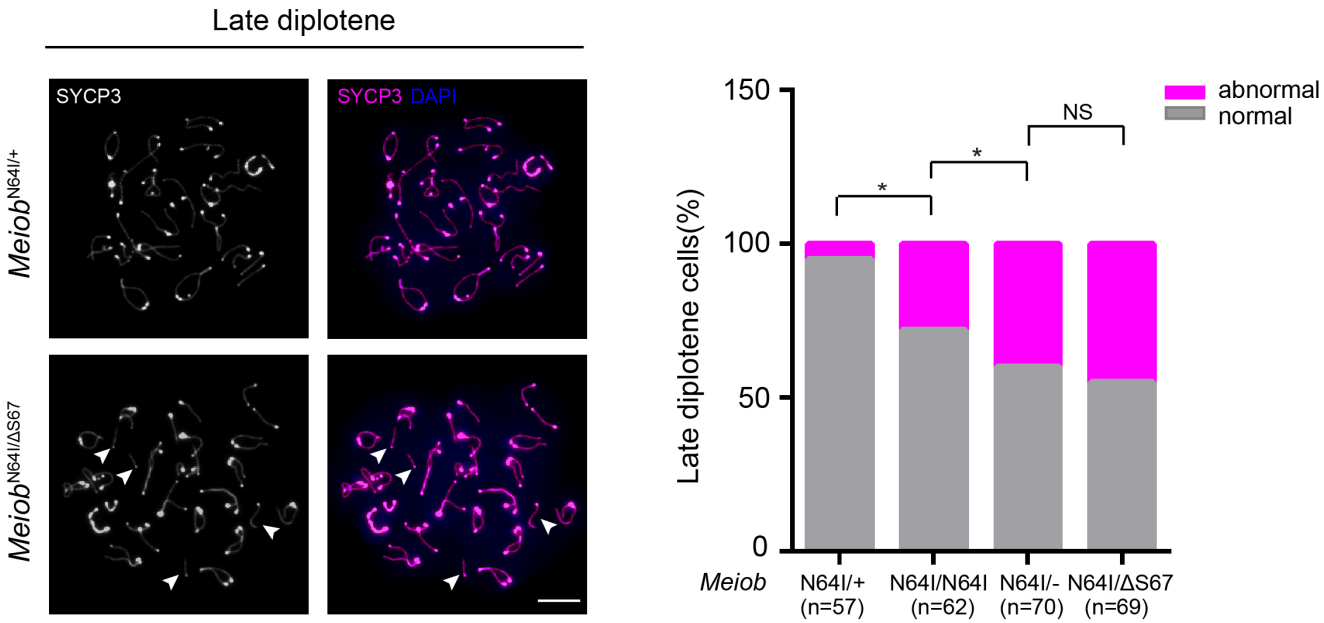

Supplementary Figure S6. Analysis of univalent chromosomes in late diplotene spermatocytes. Spermatocytes from P24 *Meiob*$^{N64I/+}$, *Meiob*$^{N64I/N64I}$, *Meiob*$^{N64I/-}$ and *Meiob*$^{N64I/\Delta S67}$ mice were immunostained with anti-SYCP3. Univalents are indicated by arrowheads. Normal spermatocytes, all bivalents; abnormal spermatocytes, the presence of at least two univalents. n, number of diplotene spermatocytes counted. Four mice per genotype were analyzed. *$P < 0.05$ by Student's *t*-test. NS, non-significant. Scale bar, 10 μm.

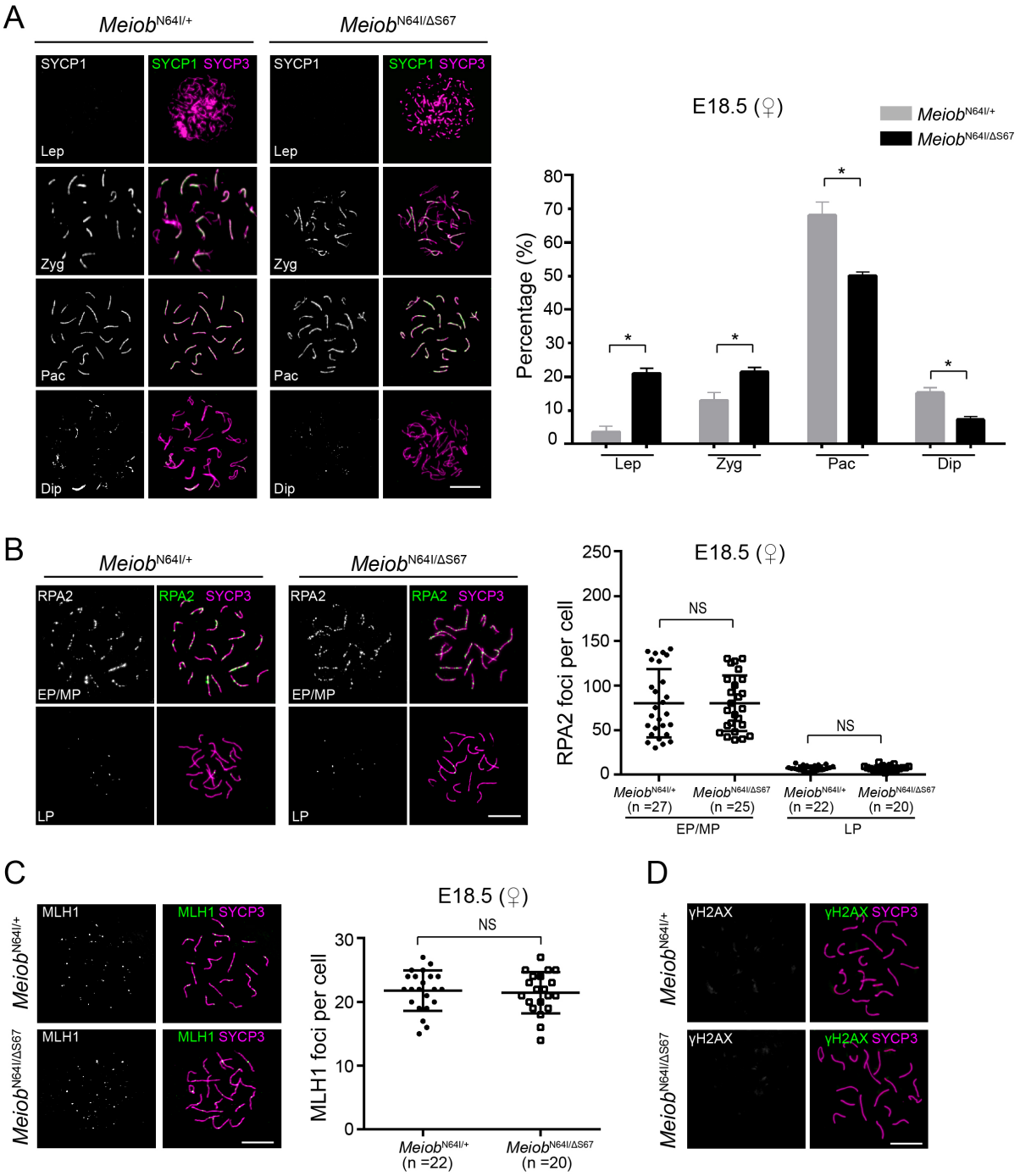

Supplementary Figure S7. *Meiob*$^{N64I/\Delta S67}$ females exhibit normal synapsis and crossover formation at prophase I. (**A**) Spread nuclei of oocytes from embryonic day 18.5 (E18.5) *Meiob*$^{N64I/+}$ and *Meiob*$^{N64I/\Delta S67}$ ovaries were immunostained with anti-SYCP1 and anti-SYCP3 antibodies. The graph shows the percentage of prophase I substages. 180 *Meiob*$^{N64I/+}$ and 150 *Meiob*$^{N64I/\Delta S67}$ oocytes from three embryos per genotype were counted. Lep, leptotene; Zyg, zygotene; Pac, pachytene; Dip, diplotene. Data are presented as mean ± S.D., *$P < 0.05$ by Student's *t*-test. (**B**) Analysis of RPA2 foci in E18.5 oocytes. n, number of oocytes. Early-pachytene (EP), Mid-pachytene (MP), late-pachytene (LP). (**C**) Analysis of MLH1 foci in *Meiob*$^{N64I/+}$and *Meiob*$^{N64I/\Delta S67}$ pachytene oocytes at E18.5. n, number of mid to late pachytene oocytes counted. Three embryos per genotype were analyzed. (**D**)

Lack of γH2AX in *Meiob*$^{N64I/+}$ and *Meiob*$^{N64I/\Delta S67}$ pachytene oocytes at E18.5. NS, non-significant. Scale bars, 10 μm.

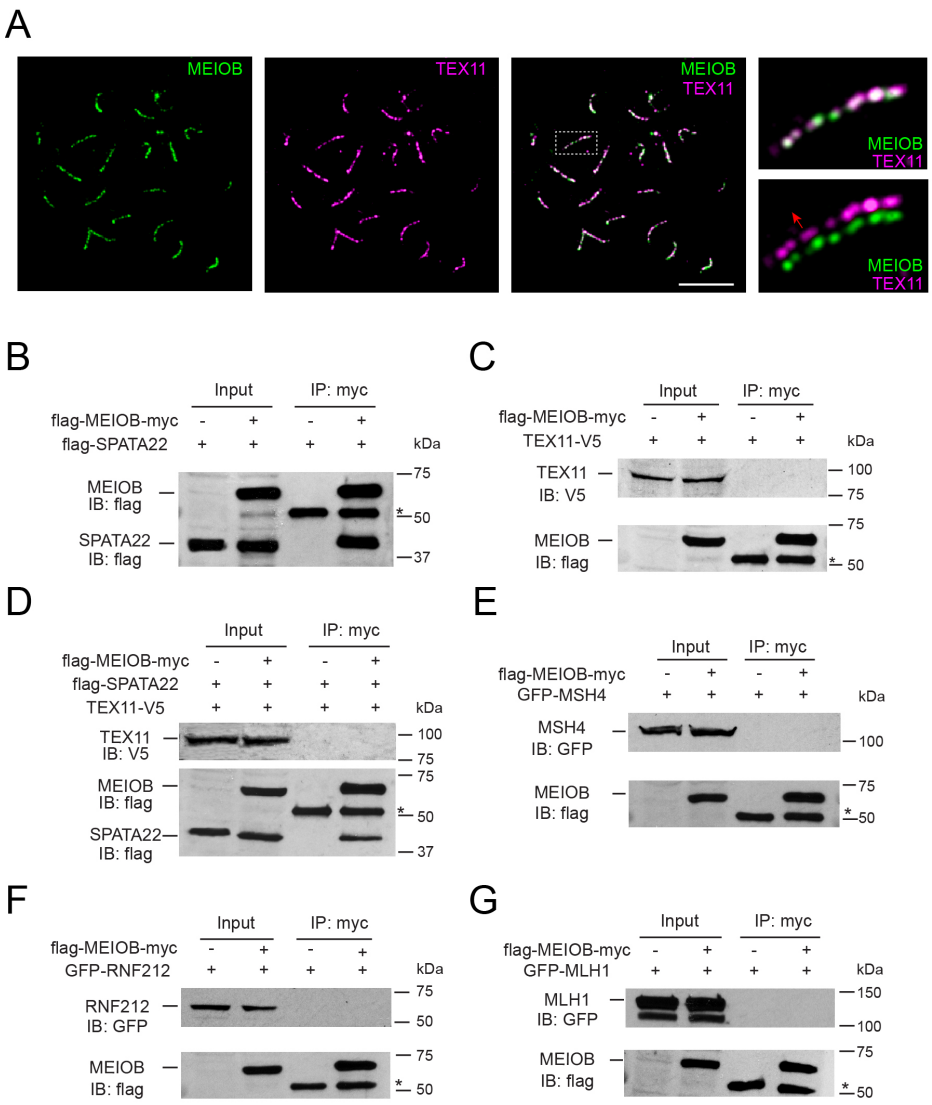

Supplementary Figure S8. Colocalization of MEIOB with TEX11 in pachytene spermatocytes and *in vitro* co-immunoprecipitation (co-IP) analyses. (**A**) Double immunostaining of spermatocytes from P20 testes was performed with guinea pig anti-MEIOB and rabbit anti-TEX11 antibodies. Enlarged views of the chromosome marked by a box (without or with offset channels) were shown. The red arrow indicates the offset direction of the red channel (TEX11). (**B-G**) HEK293T cells were transfected with the indicated expression vectors. (**B**) Co-IP of MEIOB and SPATA22 serves as a positive control. (**C, D**) Co-IP analysis of MEIOB and TEX11 interaction in the absence (**C**) or presence (**D**) of SPATA22. (**E-G**) Co-IP analysis of MEIOB with MSH4 (**E**), RNF212 (**F**), and MLH1 (**G**). ∗, antibody heavy chain.

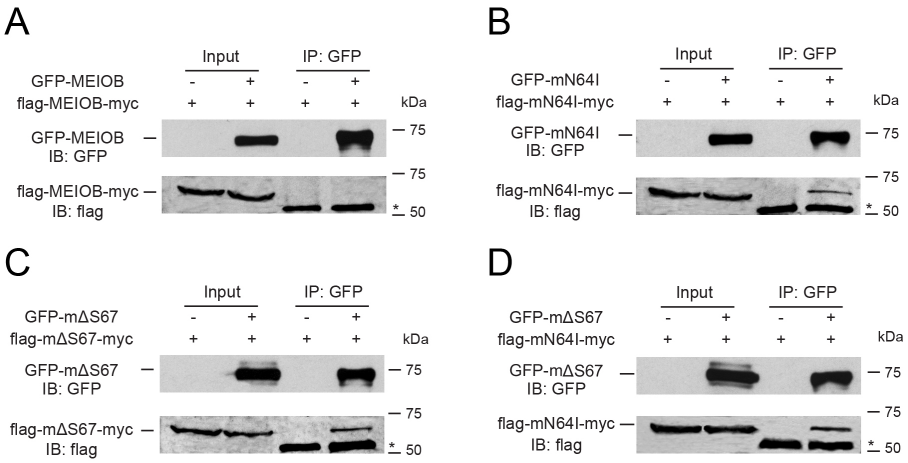

Supplementary Figure S9. *Meiob* mutations cause self-association: reciprocal immunoprecipitations with anti-GFP antibody for experiments in Figure 6. Full-length mouse MEIOB proteins were expressed in HEK293T cells in all transfection experiments. (**A**) Wild type MEIOB does not self-associate: reciprocal co-IP of Figure 6E. (**B**) MEIOB^{N64I} interacts with itself: reciprocal co-IP of Figure 6G. (**C**) MEIOB$^{\Delta S67}$ interacts with itself: reciprocal co-IP of Figure 6H. (**D**) MEIOB^{N64I} interacts with MEIOB$^{\Delta S67}$: reciprocal co-IP of Figure 6I.

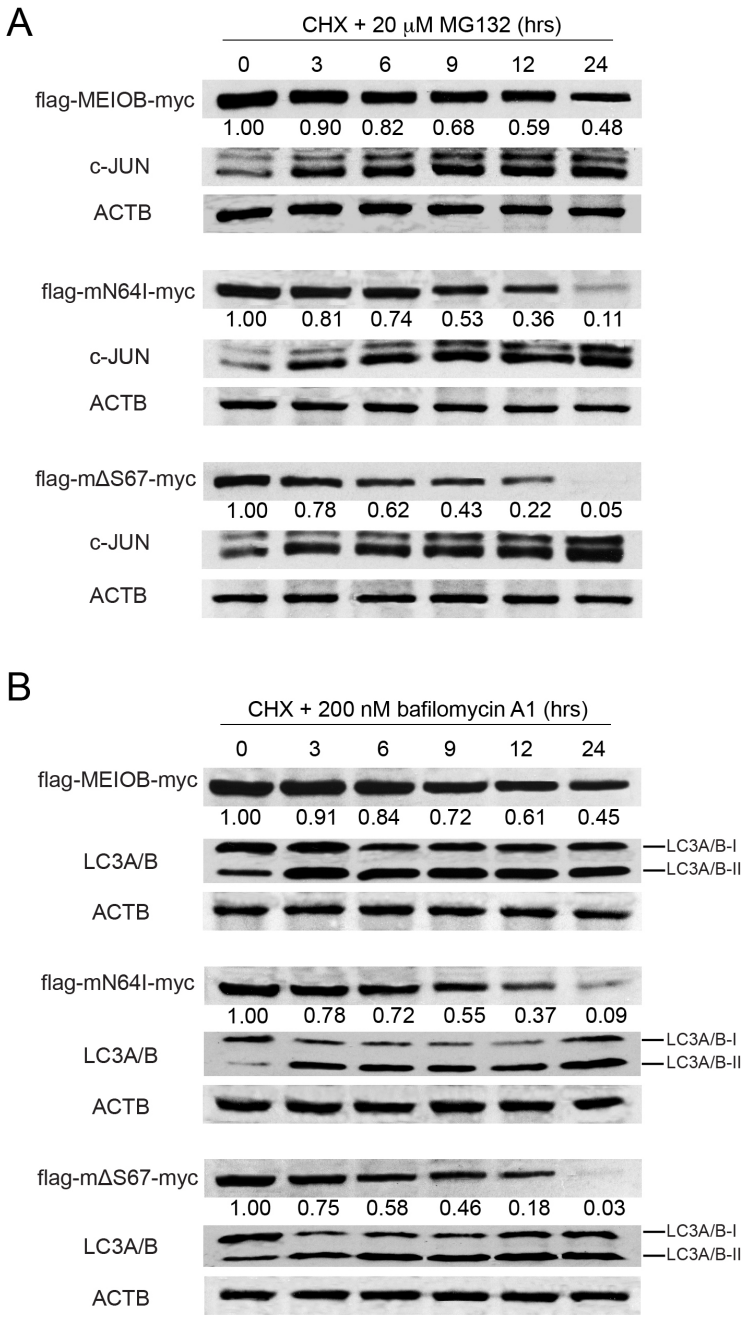

Supplementary Figure S10. MEIOB is not degraded through the proteasome or the autophagosome. **(A)** Western blot analysis of mouse MEIOB (wt), MEIOB^{N64I}, and MEIOB$^{\Delta S67}$ in HEK293T cells treated with cycloheximide and MG132. c-Jun serves as a positive control for MG132 treatment. ACTB serves as a loading control. **(B)** Western blot analysis of mouse MEIOB (wt), MEIOB^{N64I}, and MEIOB$^{\Delta S67}$ in HEK293T cells treated with cycloheximide and bafilomycin A1. LC3A/B-II, an autophagosome marker serves as a positive control for bafilomycin A1treatment. ACTB serves as a loading control. The number below each band is the fold change of protein abundance compared to the time zero. The experiments were performed twice with similar results.